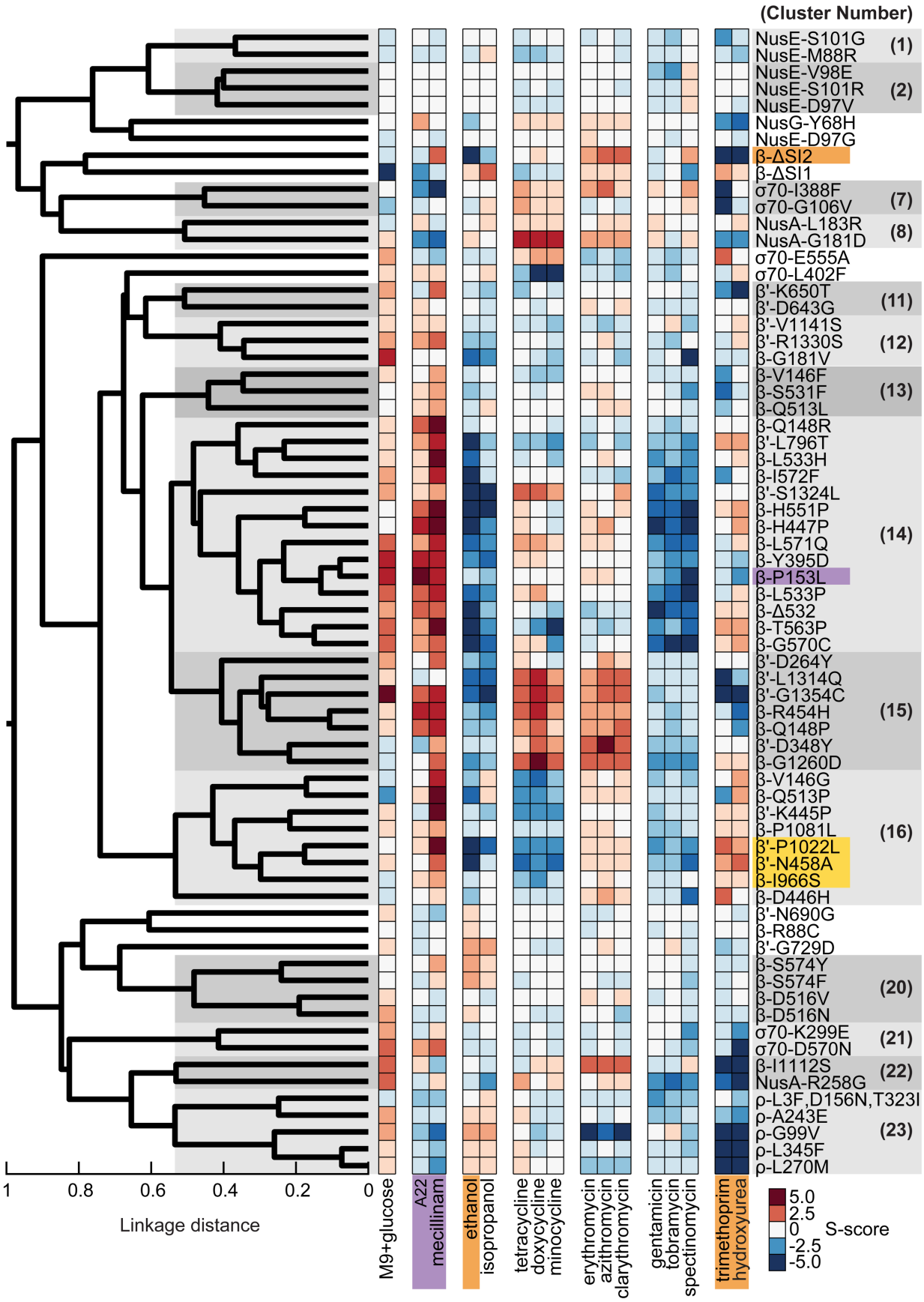
(Cluster Number)
NusE-S101G
NusE-M88R
(1)
NusE-V98E
NusE-S101R
NusE-D97V
(2)
NusG-Y68H
NusE-D97G
β-ΔSI2
β-ΔSI1
σ70-I388F
σ70-G106V
(7)
NusA-L183R
NusA-G181D
(8)
σ70-E555A
σ70-L402F
β'-K650T
β'-D643G
(11)
β'-V1141S
β'-R1330S
β-G181V
(12)
β-V146F
β-S531F
β-Q513L
(13)
β-Q148R
β'-L796T
β-L533H
β-I572F
β'-S1324L
β-H551P
β-H447P
β-L571Q
β-Y395D
β-P153L
β-L533P
β-Δ532
β-T563P
β-G570C
(14)
β'-D264Y
β'-L1314Q
β'-G1354C
β-R454H
β-Q148P
β'-D348Y
β-G1260D
(15)
β-V146G
β-Q513P
β'-K445P
β-P1081L
β'-P1022L
β'-N458A
β-I966S
(16)
β-D446H
β'-N690G
β-R88C
β'-G729D
β-S574Y
β-S574F
β-D516V
β-D516N
(20)
σ70-K299E
σ70-D570N
(21)
β-I1112S
NusA-R258G
(22)
ρ-L3F,D156N,T323I
ρ-A243E
ρ-G99V
ρ-L345F
ρ-L270M
(23)
1
0.8
0.6
0.4
0.2
0
Linkage distance
M9+glucose
A22
mecillinam
ethanol
isopropanol
tetracycline
doxycycline
minocycline
erythromycin
azithromycin
clarythromycin
gentamicin
tobramycin
spectinomycin
trimethoprim
hydroxyurea
5.0
2.5
0
-2.5
-5.0
S-score

Supplemental Figure 1: Dendrogram of significant hierarchical clusters and a heatmap of relevant chemical-genetic interactions, Related to Figures 2,3,4,5.

Transcription mutants were hierarchically clustered according to shared sensitivities in the chemical-genetic dataset. A cutoff for linkage distance (Methods) identified 14 clusters and 9 singletons within the dataset. A subset of the chemical conditions and mutations that had interesting chemical-genetic interactions were chosen for further analysis and these are highlighted with colored boxes. A22 and mecillinam (second column group from the left, purple) had widespread positive S-scores that were concentrated in, but not limited to, cluster 14. The β-P153L mutation (cluster 14, purple) was investigated further for its resistance to mecillinam and A22. Alcohol treatments (third column group from the left) had widespread negative S-scores that were concentrated in, but not limited to, cluster 14 and cluster 15. Sensitivity to select aminoglycosides (gentamicin, tobramycin, and spectinomycin; sixth column group from the left) was enriched in cluster 14 (**Figure 3B**). Resistance to tetracycline (tetracycline, doxycycline, and minocycline; fourth column group from the left) (**Figure 3C**) and macrolide (erythromycin, azithromycin, and clarithromycin; fifth column group from the left) antibiotics was enriched in cluster 15. Sensitivity to tetracyclines was enriched in cluster 16 (**Figure 3C**). Sensitivity to trimethoprim and hydroxyurea (right-most column group) was enriched in cluster 22 and cluster 23. Resistance to trimethoprim and hydroxyurea was enriched in cluster 16. Sensitivity of β-ΔSI2 (orange) to ethanol, trimethoprim, and hydroxyurea (orange) was confirmed using liquid growth curves (**Figure 4A,B**). The high correlations among β′-P1022L, β′-N458A, and β-I966S (cluster 16, yellow) were used to predict a hyper-attenuation phenotype for β′-N458A and β-I966S (**Figure 4C,D**). Resistance of β-P153L to mecillinam and A22 (**Figure 5A**) was confirmed using liquid growth curves (**Figure 6A**).

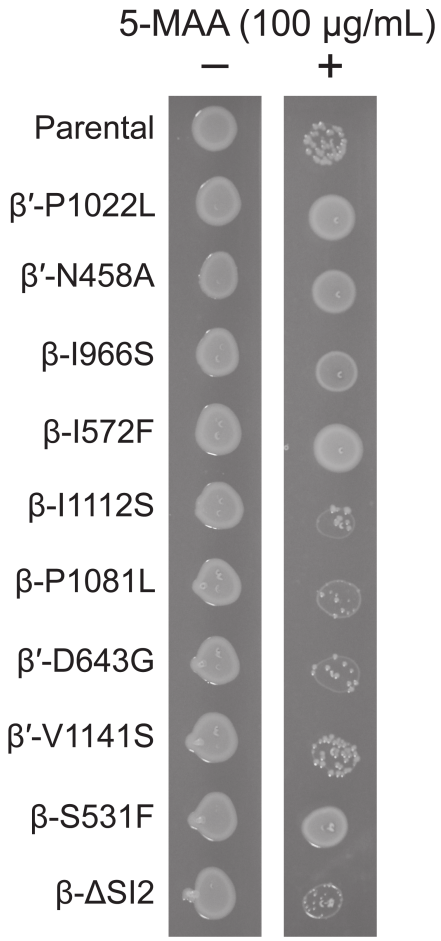

Supplemental Figure 2: 5-MAA resistance in transcription mutants, Related to Figure 4.

In a Δ*trpR* background, expression of the *trp* locus is mainly controlled by attenuation. Hyper-attenuation reduces *trp* expression and makes cells resistant to a toxic analogue of a tryptophan biosynthesis intermediate, 5-methyl anthranilic acid (5-MAA). The genotype of the parental strain (Parental) in this experiment is MG1655 *rpoBC-cat* Δ*trpR*. All other strains are derivatives of this parental strain with the specified mutation in core RNA polymerase. Mutations in β include β-I966S, β-ΔSI2, β-P1081L, and β-I1112S. Mutations in the active site/secondary channel include β′-N458A, β′-D643G, and β′-V1141S. The Rif^R mutations are β-S531F and β-I572F. Resistance to 5-MAA at 100 µg/mL is represented by consistent density throughout the 3 µL spot. Sensitive strains in this experiment show lower overall density and the occurrence of suppressors as small colonies. The $5\text{-}MAA^R$ phenotype was strongest in β′-P1022L, β′-N458A, β-I966S, β-S531F, and β-I572F.

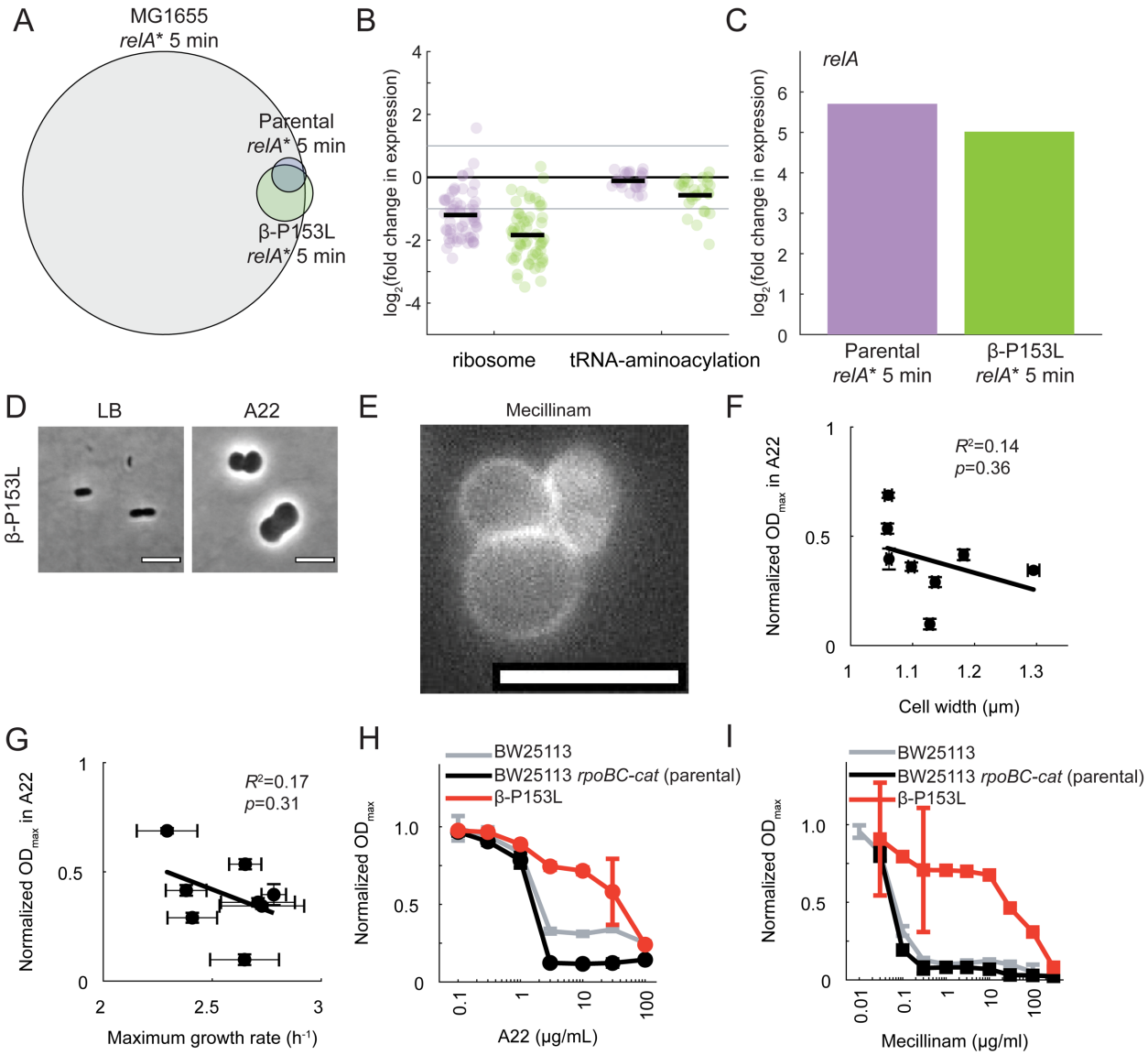

Supplemental Figure 3: Induction of *relA in β-P153L leads to repression of translation-related genes, β-P153L grows as cocci with a cell wall in A22 and mecillinam, A22 resistance among M⁺ mutants is not correlated with either cell width or growth rate, and β-P153L does not simply correct the cell elongation phenotype of its parental strain. Related to Figures 5, 6, 7.**

A) There is extensive overlap in the significantly differentially expressed genes due to induction of *relA** for 5 min in β-P153L (green, data collected in this study), the parental strain (purple, data collected in this study), and MG1655 (gray, from (Sanchez-Vazquez et al., 2019)). The reference dataset (gray) has a more extensive response than the experiments in this study.

B) β-P153L (green) and its parental strain (purple) experienced repression of ribosome-related (ribosome) and tRNA aminoacylation-related genes after induction of *relA**. These data are consistent with effects of the stringent response. Fold-changes were more pronounced in β-P153L than in the parental strain. Individual genes are plotted as circles. The set average is shown as a solid black line. Two-fold changes in expression are marked with a solid gray line.

C) The stronger effects of *relA** induction in β-P153L (**A,B**) were not due to higher expression of *relA**. Despite having a stronger repressive effect on translation-related genes, *relA* induction was slightly lower in β-P153L compared to its parental strain.

D) Although β-P153L prevents death due to A22 treatment, β-P153L cells still lost rod shape in the presence of A22. Representative phase-contrast images of log-phase β-P153L cells are shown in LB (top) and LB+15 μg/mL A22 (bottom). Scale bar: 5 μm.

E) B-P153L cells treated with mecillinam still have a cell wall and grow as cocci. Log-phase β-P153L cells grown in the presence of 15 μg/mL mecillinam were pulse-labeled with the fluorescent D-amino acid analogue HADA. Incorporation of HADA into the cell periphery demonstrated that coccoidal β-P153L cells retain a cell wall during mecillinam treatment. Scale bar: 5 μm.

F) Resistance to A22 was not correlated with cell width. The maximum OD_{600} of the 7 M^+ mutants and their parental control in LB+13.5 μg/mL A22 was extracted from growth curves and normalized by growth curves of the same strain in LB without antibiotic. The normalized OD_{max} of the 7 mutants was not correlated with the average cell width of log-phase cells grown in LB (R^2=0.14, p=0.36).

G) The normalized OD_{max} calculated as in (**F**) was not correlated with maximum growth rate extracted from growth curves of the mutants in LB without A22 (R^2=0.17, p=0.31).

H) β-P153L is highly resistant to A22, while both its parental strain (BW25113 *rpoBC-cat*) and BW25113 are susceptible. Maximum OD_{600} (OD_{max}) was extracted from growth curves of β-P153L (red), its parental control (black), and BW25113 (gray) and normalized by the OD_{max} of each strain in the absence of antibiotic. The growth

medium for all strains was LB. Error bars represent 95% confidence intervals. Data for β-P153L and the parental strain are identical to those in **Figure 6A** and are replotted here for comparison to BW25113. The parental strain halts growth earlier than BW25113 when treated with A22, but the concentration at which A22 becomes lethal is identical for the two strains within the resolution of this experiment. By contrast to both wild-type strains, β-P153L was highly resistant to A22.

I) β-P153L is highly resistant to mecillinam, while both its parental strain (BW25113 *rpoBC-cat*) and BW25113 are susceptible. Data is as in (**H**), except strains were treated with mecillinam instead of A22. The concentration at which mecillinam became lethal was identical for BW25113 and the parental strain within the resolution of this experiment. By contrast to both wild-type strains, β-P153L was highly resistant to mecillinam.

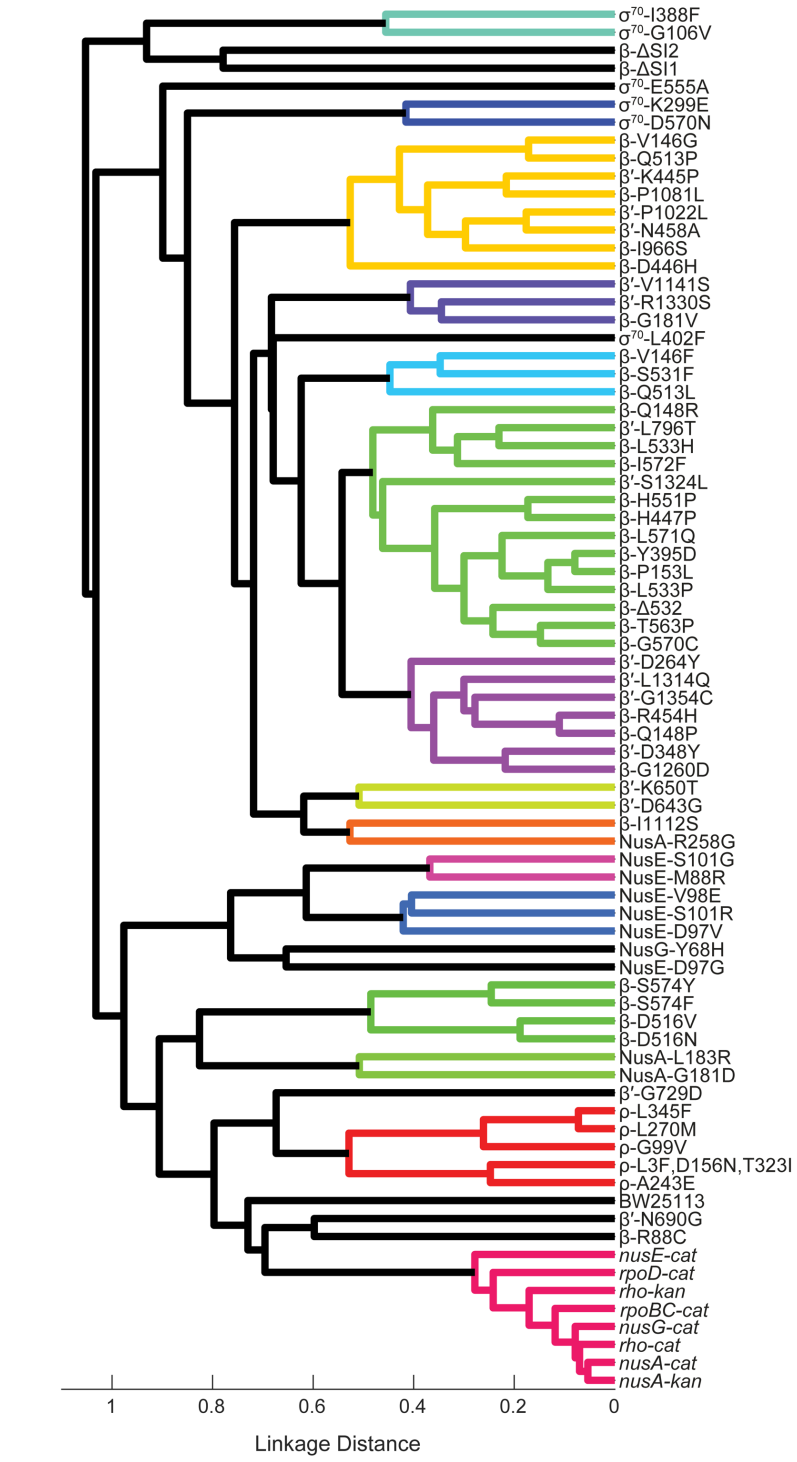

Cluster number

7	13	22	8
21	14	1	23
16	15	2	marker-only allele cluster
12	11	20	

Supplemental Figure 4: Dendrogram of transcription mutants including the marker-only alleles, Related to Quantification and Statistical Analysis in STAR Methods, subsection, Statistical analysis to generate S-scores.

Transcription mutants were hierarchically clustered according to shared sensitivities in our chemical-genetic dataset using the same approach as in **Supplemental Figure 1** (**STAR Methods**). However, in this figure the marker-only alleles were not filtered out of the dataset before hierarchical clustering. Clusters defined based on the significance threshold are colored. The cluster number corresponds to those used in the main text. Re-analysis including the marker-only alleles identified the same 14 clusters and 9 singletons of transcription mutants as in **Supplemental Figure 1**. The marker-only alleles form a single cluster (bottom of the dendrogram), while BW25113 (true wild-type) and transcription mutants β-R88C and β′-N690C are grouped as singleton outliers.

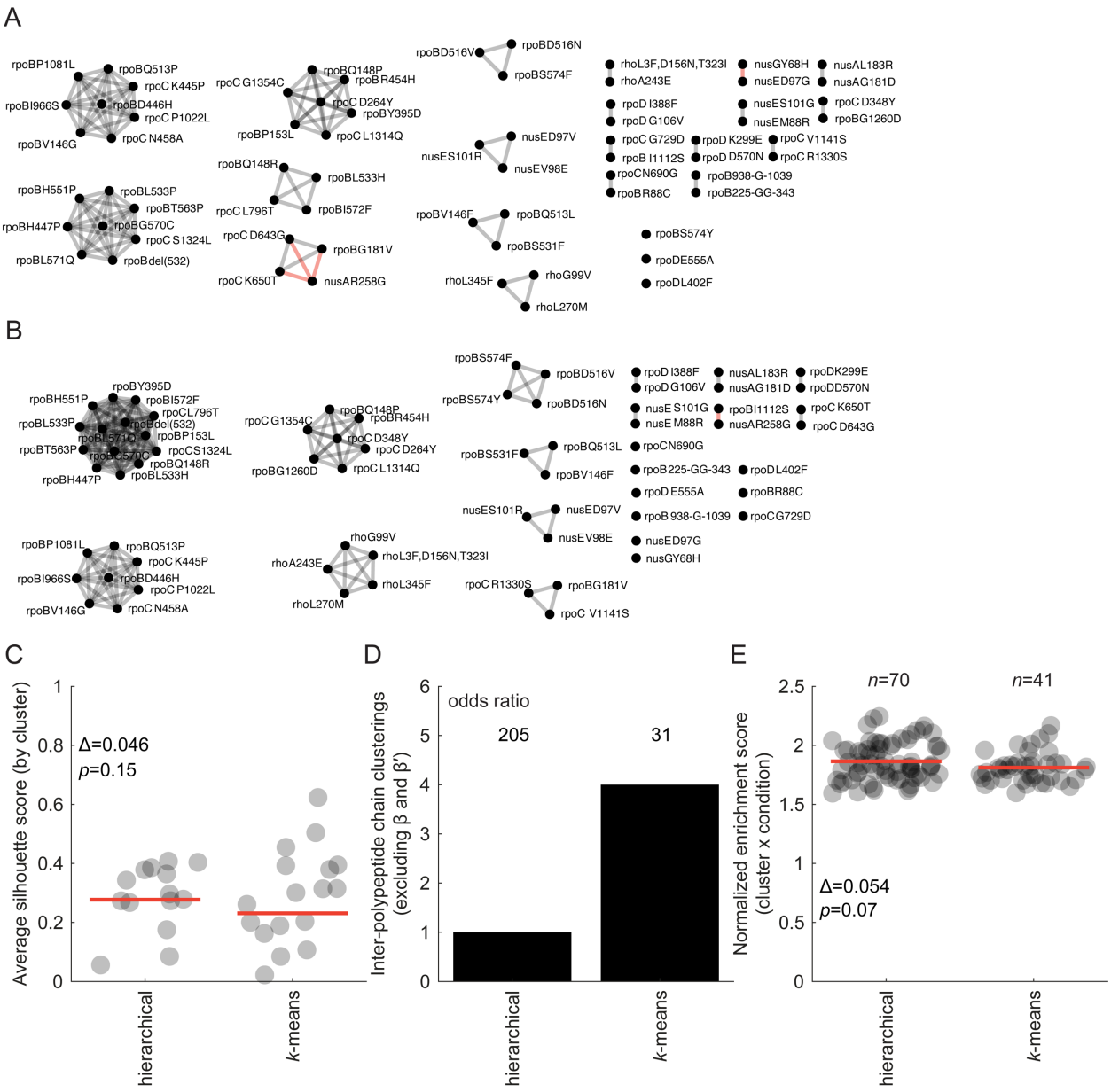

Supplemental Figure 5: *k*-means clustering of the transcription mutants using *k*=23, Related to Quantification and Statistical Analysis in STAR Methods, subsection, Defining and visualizing clusters. Results of clustering methods are compared

A) The results from using the number of "clusters" (14 clusters + 9 singletons, *k*=23) defined by hierarchical clustering as an input to a k-means clustering algorithm. The best solution from 10,000 iterations is shown. There are more clusters of a smaller size in core RNA polymerase. There are more inter-polypeptide chain clustering pairs outside of β and β′. These are highlighted with red edges. There

are fewer singletons. However, quantitative comparison between the two clustering approaches reveals that there is reasonable overlap in the results, with an adjusted mutual information score of 0.70.

B) For comparison, the clusters identified in the paper are shown. These clusters were identified using hierarchical clustering and a statistically defined cutoff.

C) The average silhouette scores are plotted for the hierarchical and k-means approaches. Plotted circles are the average silhouette score for a cluster. The red lines are the average silhouette score across the entire dataset. The total average difference between clustering methods is 0.046 (p=0.15).

D) The number of pair-wise co-clustering interactions involving mutations in different polypeptide chains (that don't include β and β′) are plotted as bar plots. For the k-means, there are 4 pairwise interactions, 3 of which come from the co-clustering of NusA-R258G with mutations in the core polymerase (**A**). In the hierarchical clustering dataset, the sole inter-chain clustering interaction is that between NusA-R258G and β-I1112S (**B**). Above each bar plot is the odds ratio (*OR*) for overlap between mutations co-clustering and occurring in the same polypeptide chain (*OR*=205 for hierarchical and *OR*=31 for *k*-means clustering).

E) GSEA was used to look for enrichments of S-scores in particular conditions within the clusters defined by the two methods. If the multiple-hypothesis-corrected p value was less than 0.05, the enrichment was considered significant and the value of its normalized enrichment score (NES) is plotted. There are more significant enrichments for hierarchical (n=70) compared to k-means (n=41) clustering, and the average NES is 0.054 higher for hierarchical clustering (p=0.07).

Supplemental Tables

Supplemental Table 2: Conditions used in screen, Related to Figure 1.

Stress condition *	Concentration (current screen)	Concentration (matched condition from Keio library)
1-Butanol	1% (v/v)	1% (v/v)
10 °C	N.A.	N.A.
25 °C	N.A.	N.A.
A22	5 µg/mL	5 µg/mL
Amoxicillin	1.5 µg/mL	1.5 µg/mL
Ampicillin	4 µg/mL	4 µg/mL
Azelaic acid	1 mg/mL	1 mg/mL
Azidothymidine	2.5 ng/mL	500 pg/mL
Azithromycin	1 µg/mL	1 µg/mL
Bicyclomycin	20 µg/mL	20 µg/mL
Bile salts	2% (w/v)	2% (w/v)
Blasticidin S	33 µg/mL	33 µg/mL
Bleomycin	500 ng/mL	1 µg/mL
Carbonyl cyanide *m*-chlorophenyl hydrazine (CCCP)	2 µg/mL	2 µg/mL
Cefaclor	2 µg/mL	3 µg/mL
Cefoxitin	500 ng/mL	750 ng/mL
Cefsulodin	24 µg/mL	12 µg/mL
Chlorhexidine	5 µg/mL	5 µg/mL
Cinoxacin	3 µg/mL	3 µg/mL
Ciprofloxacin	1 ng/mL	1 ng/mL
Clarythromycin	5 µg/mL	5 µg/mL
Copper(II)	2 mM	2 mM
Deoxycholic acid	1% (w/v)	1% (w/v)
Dibucaine	1.2 mM	800 µM
Dimethyl sulfoxide (DMSO)	9.5% (v/v)	9.5% (v/v)
Doxycycline	750 ng/mL	750 ng/mL
Erythromycin	5 µg/mL	5 µg/mL
Ethanol	4% (w/v)	6% (w/v)
Ethidium bromide	50 µg/mL	50 µg/mL
Ethylene glycol-bis(β-aminoethyl ether)-*N,N,N′,N′*-tetraacetic acid (EGTA)	1 mM	1 mM
Ethylenediaminetetraacetic acid (EDTA)	1 mM	1 mM
Fusidic acid	50 µg/mL	50 µg/mL
Gentamicin	100 ng/mL	50 ng/mL
Gliotoxin	10 µg/mL	10 µg/mL
Guanidine hydrochloride	30 mM	30 mM
Holomycin	2.5 µg/mL	2.5 µg/mL
Hydroxyurea	5 mM	5 mM
Isopentanol	0.5% (v/v)	0.5% (v/v)
Isopropanol	5% (v/v)	5% (v/v)
Kasugamycin	20 µg/mL	20 µg/mL
M9 minimal media 0.2% glucose with 5-fluorouridine	250 ng/mL	250 ng/mL
M9 minimal media 0.2% glucose with 5-methylanthranilic acid	20 µg/mL	20 µg/mL
M9 minimal media 0.2% glucose with 5-methyltryptophan	20 µg/mL	20 µg/mL
M9 minimal media 0.2% glucose with casamino acids	0.4% (w/v)	0.4% (w/v)
M9 minimal media 0.2% glucose with UV	12 sec	12 sec
M9 minimal media with acetate	0.6% (w/v)	0.6% (w/v)
M9 minimal media with glucosamine	0.2% (w/v)	0.2% (w/v)
M9 minimal media with glucose	0.2% (w/v)	0.2% (w/v)
M9 minimal media with glycerol	0.4% (w/v)	0.4% (w/v)
M9 minimal media with maltose	0.1% (w/v)	0.1% (w/v)
M9 minimal media with succinate	0.3% (w/v)	0.3% (w/v)
Mecillinam	120 ng/mL	120 ng/mL

Minocycline	1 μg/mL	1 μg/mL
Nalidixic acid	1.5 μg/mL	1 μg/mL
Nitrofurantoin	1.5 μg/mL	2 μg/mL
Novobiocin	12 μg/mL	30 μg/mL
Phenazine methosulfate	100 μM	50 μM
Phenol	0.1% (v/v)	0.1% (v/v)
Polymyxin B	4 μg/mL	2 μg/mL
Procaine	30 mM	30 mM
Pseudomonic acid A	36 μg/mL	36 μg/mL
Pyocyanin	10 μg/mL	10 μg/mL
Rifampicin	4 μg/mL	4 μg/mL
SDS and EDTA combination treatment	0.5% (w/v) (SDS); 500 μM (EDTA)	0.5% (w/v) (SDS); 500 μM (EDTA)
Serine hydroxamate	600 μg/mL	600 μg/mL
Silver(II)	1 μM	1 μM
Sodium chloride	330 mM	450 mM
Sodium dodecyl sulfate (SDS)	1% (w/v)	1% (w/v)
Sodium fluoride	100 mM	100 mM
Spectinomycin	4 μg/mL	6 μg/mL
Spiramycin	20 μg/mL	20 μg/mL
Streptonigrin	500 ng/mL	500 ng/mL
Sulfamonomethoxine	100 μg/mL	100 μg/mL
tert-Butyl alcohol	5% (v/v)	5% (v/v)
Tetracycline	500 ng/mL	500 ng/mL
Thiolutin	7 μg/mL	7 μg/mL
Tobramycin	50 ng/mL	100 ng/mL
Trimethoprim	100 ng/mL	300 ng/mL
Tunicamycin	7.5 μg/mL	7.5 μg/mL
Urea	750 mM	750 mM
Urea	320 mM	320 mM
Irradiation with ultraviolet light (UV)	12 sec	6 sec
Vancomycin	50 μg/mL	50 μg/mL

Antibiotics were added to agar plates at the specified concentration and colony arrays were pinned onto the solid agar surface. *: Unless otherwise noted, the medium used was LB and the growth temperature was 37 ˚C. N.A.: Not applicable.

Supplemental Table 3: Conditional enrichments among transcription mutant clusters and pre-defined classes, Related to Figures 3,5.

Condition	NES	p-value (adjusted)	Individually significant
Cluster2			
No significant enrichments			
Cluster12			
No significant enrichments			
Cluster13			
No significant enrichments			
Cluster14			
Chlorhexidine	-2.1	0.00	2
Azelaic acid	-2.02	0.00	8
Spectinomycin	-2.01	0.00	8
Gentamicin	-1.94	0.00	5
Tobramycin	-1.84	3.58×10^{-3}	7
Silver(II)	-1.82	0.00	3
Copper(II)	-1.76	2.03×10^{-2}	4
Holomycin	-1.75	3.04×10^{-2}	1
Polymyxin B	-1.74	1.00×10^{-2}	8
Isopropanol	-1.74	1.15×10^{-2}	6
25 °C	-1.71	1.11×10^{-2}	10
M9 minimal media 0.2% glucose with casamino acids	-1.7	1.88×10^{-2}	8
Tunicamycin	-1.68	0.00	7
Ethanol	-1.66	8.21×10^{-3}	11
1-Butanol	-1.61	2.00×10^{-2}	4
M9 minimal media with glycerol	1.62	4.03×10^{-2}	3
M9 minimal media with maltose	1.64	4.75×10^{-2}	7
M9 minimal media with glucosamine	1.66	2.37×10^{-2}	6
M9 minimal media with succinate	1.79	9.89×10^{-3}	6
M9 minimal media 0.2% glucose with 5-fluorouridine	1.82	2.21×10^{-2}	2
M9 minimal media 0.2% glucose with 5-methyltryptophan	1.82	9.94×10^{-3}	2
Phenazine methosulfate	1.85	1.55×10^{-2}	3
Bleomycin	1.95	0.00	1
Mecillinam	1.96	3.97×10^{-3}	12
A22	2.08	0.00	5
Cluster15			
Isopentanol	-1.79	2.03×10^{-2}	1
tert-Butyl alcohol	-1.7	3.04×10^{-2}	2
Azithromycin	1.73	9.94×10^{-3}	1
Guanidine hydrochloride	1.77	1.61×10^{-2}	2
Pseudomonic acid A	1.82	9.38×10^{-3}	5
Tetracycline	1.85	3.04×10^{-2}	1
Doxycycline	1.99	0.00	4
Cluster16			
Tetracycline	-1.97	1.00×10^{-2}	1
Pseudomonic acid A	-1.82	2.42×10^{-2}	3
Serine hydroxamate	-1.82	2.00×10^{-2}	2
Doxycycline	-1.77	2.73×10^{-2}	1
Sulfamonomethoxine	2.08	0.00	1
Cluster20			
Rifampicin	1.61	7.91×10^{-3}	4
Chlorhexidine	1.72	4.75×10^{-2}	1
Cluster23			
Rifampicin	-2.03	0.00	4
Mecillinam	-2	4.08×10^{-2}	1
Sodium fluoride	-1.91	2.73×10^{-2}	3
Ciprofloxacin	-1.86	1.00×10^{-2}	1
Ethidium bromide	-1.81	3.04×10^{-2}	2

Azidothymidine	-1.75	3.04×10^{-2}	2
Spiramycin	-1.72	3.40×10^{-2}	1
Dibucaine	-1.63	3.18×10^{-2}	1
Bicyclomycin	-1.6	1.25×10^{-2}	5
Cinoxacin	1.66	3.95×10^{-2}	1
M+			
tert-Butyl alcohol	-2.16	0.00	2
Holomycin	-2.14	0.00	2
Isopropanol	-2.08	0.00	8
Isopentanol	-2.02	4.10×10^{-3}	1
Polymyxin B	-2.01	0.00	9
25 °C	-1.88	0.00	13
Chlorhexidine	-1.86	3.40×10^{-2}	2
10 °C	-1.8	6.04×10^{-3}	7
1-Butanol	-1.78	0.00	9
M9 minimal media 0.2% glucose with casamino acids	-1.75	1.25×10^{-2}	10
Azelaic acid	-1.73	1.90×10^{-2}	7
Tunicamycin	-1.72	0.00	8
Silver(II)	-1.71	2.03×10^{-2}	4
Spectinomycin	-1.63	3.04×10^{-2}	8
Ethanol	-1.56	2.87×10^{-2}	10
M9 minimal media 0.2% glucose with 5-methyltryptophan	1.65	4.57×10^{-2}	4
M9 minimal media with glycerol	1.68	2.03×10^{-2}	3
Bleomycin	1.73	3.40×10^{-2}	1
M9 minimal media 0.2% glucose with 5-methylanthranilic acid	1.77	1.90×10^{-2}	9
Mecillinam	1.83	1.00×10^{-2}	10
Guanidine hydrochloride	1.88	4.82×10^{-3}	2
Pseudomonic acid A	1.89	2.03×10^{-2}	9
M9 minimal media with glucosamine	1.91	0.00	7
M9 minimal media with succinate	1.91	0.00	7
M9 minimal media with maltose	1.92	0.00	8
Doxycycline	1.99	5.49×10^{-3}	4
Tetracycline	1.99	1.55×10^{-2}	1
A22	2.06	0.00	7
5-MAA^{R}			
No significant enrichments			
Ethanol-tolerant			
Sodium fluoride	-1.96	1.52×10^{-2}	3
Sulfamonomethoxine	-1.9	0.00	1
Azidothymidine	-1.81	2.73×10^{-2}	1
Hydroxyurea	-1.6	2.42×10^{-2}	4
Urea	-1.58	4.57×10^{-2}	4
Trimethoprim	-1.57	3.02×10^{-2}	5
GalR			
No significant enrichments			
Mpa			
No significant enrichments			

Condition: name of the stressor. **NES:** normalized enrichment score as output by GSEA v. 3.0. Larger magnitude scores indicate higher enrichment. Negative NES values correspond to enrichment for negative S-scores. Positive NES values correspond to enrichment for positive S-scores. Enriched conditions are sorted according to NES. **p-value (adjusted):** Benjamini-Hochberg FDR-corrected p-values (corrected from nominal p-values output by GSEA). **Individually significant:** Significant S-scores were defined using an independent method to GSEA using a cut-off that controlled the FDR at 5% (Methods) (Nichols et al., 2011). The number of mutations within the class that were significant according to this metric are listed. A cluster-chemical enrichment with high NES but few individually significant mutations may reflect a clear and statistically significant enrichment for low-magnitude S-scores within the mutant cluster. Alternatively, the enrichment may be driven by a subset of mutants within the cluster with high-magnitude S-scores. Cluster numbers being analyzed are as shown in **Figure 2B** and **Supplemental Figure 1**. **M+:** The class of M+

mutants. **5-MAA^{R}:** The class of known hyper-attenuation mutants, as defined by resistance to 5-methyl-anthranilic acid in a Δ*trpR* background. **Ethanol-tolerant:** Mutations found in strains evolved for tolerance to ethanol. **GalR:** suppression of galactose sensitivity in *gal10*Δ*56* in RNA polymerase II from *Saccharomyces cerevisiae*. **Mpa:** mycophenolic acid sensitivity in RNA polymerase II from *Saccharomyces cerevisiae*.

Supplemental Table 4: Mutations detected in whole genome resequencing of Δ*mreB* strains, Related to Figure 6.

Position	Mutation	Annotation	Gene	Description	Notes
CAG67202, *rpoBC-cat*. Parental strain: BW25113 (CAG67001)					
1,484,419	Δ9 bp	pseudogene (544-552/1001 nt)	*gapC* ←	pseudogene, GAP dehydrogenase; glyceraldehyde-3-phosphate dehydrogenase (second fragment)	SNP
4,029,087	A→T	noncoding (197/1542 nt)	*rrsA* →	16S ribosomal RNA of rrnA operon	SNP
4,175,201	+T	coding (4029/4029 nt)	*rpoB* →	RNA polymerase, beta subunit	SNP associated with *cat* marker insertion
4,175,845	+A	coding (609/639 nt)	*cat* →		SNP associated with *cat* marker insertion
4,175,857	+T	coding (621/639 nt)	*cat* →		SNP associated with *cat* marker insertion
4,175,978	+A	intergenic (+103/-20)	*cat* → / → *rpoC*	–/RNA polymerase, beta prime subunit	SNP associated with *cat* marker insertion
CAG67104 *rpoBC-cat* Δ*mreB*. Parental strain: CAG67202					
1,484,419	Δ9 bp	pseudogene (544-552/1001 nt)	*gapC* ←	pseudogene, GAP dehydrogenase; glyceraldehyde-3-phosphate dehydrogenase (second fragment)	parental SNP
4,029,087	A→T	noncoding (197/1542 nt)	*rrsA* →	16S ribosomal RNA of rrnA operon	parental SNP
4,175,201	+T	coding (4029/4029 nt)	*rpoB* →	RNA polymerase, beta subunit	parental SNP
4,175,845	+A	coding (609/639 nt)	*cat* →		parental SNP
4,175,857	+T	coding (621/639 nt)	*cat* →		parental SNP
4,175,978	+A	intergenic (+103/-20)	*cat* → / → *rpoC*	–/RNA polymerase, beta prime subunit	parental SNP
3393996-3394395	Δ400	missing coverage	*mreB*	cell wall structural complex MreBCD, actin-like component MreB	Δ*mreB*::kan
CAG67105 *rpoBC-cat* Δ*mreB*. Parental strain: CAG67202					
1,484,419	Δ9 bp	pseudogene (544-552/1001 nt)	*gapC* ←	pseudogene, GAP dehydrogenase; glyceraldehyde-3-phosphate dehydrogenase (second fragment)	parental SNP
4,029,087	A→T	noncoding (197/1542 nt)	*rrsA* →	16S ribosomal RNA of rrnA operon	parental SNP
4,175,201	+T	coding (4029/4029 nt)	*rpoB* →	RNA polymerase, beta subunit	parental SNP
4,175,845	+A	coding (609/639 nt)	*cat* →		parental SNP
4,175,857	+T	coding (621/639 nt)	*cat* →		parental SNP
4,175,978	+A	intergenic (+103/-20)	*cat* → / → *rpoC*	–/RNA polymerase, beta prime subunit	parental SNP

3394017-3394392	Δ376	missing coverage	*mreB*	cell wall structural complex MreBCD, actin-like component MreB	Δ*mreB*::kan
CAG68095 β-P153L. Parental strain: CAG67202					
1,484,419	Δ9 bp	pseudogene (544-552/1001 nt)	*gapC* ←	pseudogene, GAP dehydrogenase; glyceraldehyde-3-phosphate dehydrogenase (second fragment)	parental SNP
4,029,087	A→T	noncoding (197/1542 nt)	*rrsA* →	16S ribosomal RNA of rrnA operon	parental SNP
4,171,630	C→T	P153L (CCG→CTG)	*rpoB* →	RNA polymerase, beta subunit	β-P153L
4,175,201	+T	coding (4029/4029 nt)	*rpoB* →	RNA polymerase, beta subunit	parental SNP
4,175,845	+A	coding (609/639 nt)	*cat* →		parental SNP
4,175,857	+T	coding (621/639 nt)	*cat* →		parental SNP
4,175,978	+A	intergenic (+103/-20)	*cat* → / → *rpoC*	–/RNA polymerase, beta prime subunit	parental SNP
CAG67106 β-P153L Δ*mreB*. Parental strain: CAG68095					
1,484,419	Δ9 bp	pseudogene (544-552/1001 nt)	*gapC* ←	pseudogene, GAP dehydrogenase; glyceraldehyde-3-phosphate dehydrogenase (second fragment)	parental SNP
3,430,056	G→A	E60E (GAG→GAA)	*trkA* →	NAD-binding component of TrK potassium transporter	SNP in BW2592 genetically linked to *mreB*
4,029,087	A→T	noncoding (197/1542 nt)	*rrsA* →	16S ribosomal RNA of rrnA operon	parental SNP
4,171,630	C→T	P153L (CCG→CTG)	*rpoB* →	RNA polymerase, beta subunit	parental SNP
4,175,201	+T	coding (4029/4029 nt)	*rpoB* →	RNA polymerase, beta subunit	parental SNP
4,175,845	+A	coding (609/639 nt)	*cat* →		parental SNP
4,175,857	+T	coding (621/639 nt)	*cat* →		parental SNP
4,175,978	+A	intergenic (+103/-20)	*cat* → / → *rpoC*	–/RNA polymerase, beta prime subunit	parental SNP
3393999-3394409	Δ411	missing coverage	*mreB*	cell wall structural complex MreBCD, actin-like component MreB	Δ*mreB*::kan
CAG67107 β-P153L Δ*mreB*. Parental strain: CAG68095					
1,484,419	Δ9 bp	pseudogene (544-552/1001 nt)	*gapC* ←	pseudogene, GAP dehydrogenase; glyceraldehyde-3-phosphate dehydrogenase (second fragment)	parental SNP
3,430,056	G→A	E60E (GAG→GAA)	*trkA* →	NAD-binding component of TrK potassium transporter	SNP in BW2592 genetically linked to *mreB*

3,467,784	T→C	K43R (AAA→AGA)	*rpsL* ←	30S ribosomal subunit protein S12	SNP in BW2592 genetically linked to *mreB*
4,029,087	A→T	noncoding (197/1542 nt)	*rrsA* →	16S ribosomal RNA of rrnA operon	parental SNP
4,171,630	C→T	P153L (CCG→CTG)	*rpoB* →	RNA polymerase, beta subunit	parental SNP
4,175,201	+T	coding (4029/4029 nt)	*rpoB* →	RNA polymerase, beta subunit	parental SNP
4,175,845	+A	coding (609/639 nt)	*cat* →		parental SNP
4,175,857	+T	coding (621/639 nt)	*cat* →		parental SNP
4,175,978	+A	intergenic (+103/-20)	*cat* → / → *rpoC*	–/RNA polymerase, beta prime subunit	parental SNP
3393993-3394395	Δ403	missing coverage	*mreB*	cell wall structural complex MreBCD, actin-like component MreB	Δ*mreB*::kan

Position: Genomic position of the detected mutation. **Mutation:** Identity of the detected mutation. **Annotation:** Class of mutation detected (amino acid change, coding, intergenic, or missing coverage). **Gene:** Gene affected by the mutation (or those nearby if intergenic). **Description:** Description of the affected gene. **Notes:** Annotation for the source of the detected SNP (parental SNP, derived from the BW2592 donor strain, or a true mutation).

Supplemental Table 5: Differential gene expression in β-P153L for genes of interest, Related to Figure 7.

Gene name	Accession	log2(fold change in β-P153L)	*p*-value (adjusted)
UDP-glucose/OpgH			
pgm	b0688	0.179	7×10^{-1}
rfbA	b2039	-0.056	9×10^{-1}
glgC	b3430	0.180	7×10^{-1}
galU	b1236	0.120	8×10^{-1}
galE	b0759	0.062	9×10^{-1}
galT	b0758	0.133	6×10^{-1}
otsA	b1896	-0.024	1×10^{0}
ugd	b2028	-0.184	7×10^{-1}
opgG	b1048	-0.121	8×10^{-1}
Divisome			
ftsI	b0084	0.197	6×10^{-1}
murE	b0085	0.100	8×10^{-1}
murF	b0086	0.243	3×10^{-1}
mraY	b0087	0.476	1×10^{-1}
murD	b0088	0.070	9×10^{-1}
ftsW	b0089	0.296	2×10^{-1}
murG	b0090	0.167	6×10^{-1}
murC	b0091	0.690	3×10^{-4}
ftsQ	b0093	-0.036	9×10^{-1}
ftsA	b0094	0.433	1×10^{-2}
ftsZ	b0095	0.751	3×10^{-4}
mrcB	b0149	-0.301	2×10^{-1}
dacA	b0632	0.120	8×10^{-1}
ftsK	b0890	0.068	9×10^{-1}
lpoB	b1105	0.024	1×10^{0}
zipA	b2412	0.262	3×10^{-1}
amiA	b2435	-0.045	9×10^{-1}
ftsB	b2748	-0.620	2×10^{-1}
amiC	b2817	-0.019	1×10^{0}
zapA	b2910	0.167	8×10^{-1}
ftsX	b3462	-0.415	2×10^{-1}
ftsE	b3463	0.091	9×10^{-1}
zapB	b3928	-1.698	2×10^{-5}
ftsN	b3933	-0.216	4×10^{-1}
murB	b3972	-0.392	1×10^{-1}
amiB	b4169	-0.005	1×10^{0}

Gene name: Gene in question. **Accession:** Unique identifier for gene in question. **$\log_2$(fold change in β-P153L):** $\log_2$-transformed fold-change values of read counts for β-P153L normalized to the parental control, as calculated by DESeq2 (Love et al., 2014). **p-value (adjusted):** Multiple hypothesis-corrected *p*-value for the fold change, as calculated by DESeq2 (Love et al., 2014).